Biomedical Signal Processing and Control 56 (2020) 101672

Contents lists available at ScienceDirect

Biomedical Signal Processing and Control

journal homepage: www.elsevier.com/locate/bspc

Multi-scale classification of single-cell gel electrophoresis assay using deep learning algorithm

Aykut Erdamar, Mehmet Feyzi Aksahin*

Biomedical Engineering Department, Faculty of Engineering, Baskent University, Baglica Campus, 06790, Etimesgut, Ankara, Turkey

ARTICLE INFO

Article history:
Received 17 June 2019
Received in revised form 21 August 2019
Accepted 16 September 2019

Keywords:
Comet assay
Image classification
Convolution neural network

ABSTRACT

Structural and functional integrity of deoxyribonucleic acid (DNA) is crucial for the maintenance of hereditary information. However, by-products of cellular metabolism and physical or chemical factors may cause spontaneous DNA damage. The alkaline single-cell gel electrophoresis or comet assay analysis is an easy and reliable method for the determination genotoxic effects of chemical and physical factors. Simply, it is the electrophoretic analysis of intact/damaged DNA of a single cell on in a thin layer of agarose gel. The quantitative analysis of the comet assay images is performed manually by an expert researcher. In visual scoring, DNA nuclei are scored as 0, 1, 2, 3, and 4; and the correct scoring is crucial for the determination of the DNA damage. However, visual scoring depends on the professional experience of the researcher and it is a time consuming and exhausting task. Therefore, this evaluation is inevitable to have subjective results. To avoid this subjectivity and to show the effectiveness of deep learning algorithm on cell images, a Convolution Neural Network (CNN) based deep learning method is proposed to classify comet assay images. According to the results, CNN is trained and tested with high accuracy. The results show that CNN algorithm can successfully classify five different scores of comet assay images, and these results can also reduce the subjectivity.

1. Introduction

Deoxyribonucleic acid (DNA), the hereditary material of the cell, is the polymer of deoxyribonucleotide subunits [1]. Structural and functional integrity of DNA is crucial for the maintenance of hereditary information. However, by-products of cellular metabolism and physical or chemical factors may cause spontaneous DNA damage [2]. Such DNA lesions can inhibit replication and transcription. In consequence, unrepaired lesions may lead to lethal mutations or large-scale genomic errors that threaten cellular metabolism and organism.

DNA damage analysis, in addition to information about the pathophysiology of the disease, provides important information on the early biological effects of exposure to occupationally harmful chemicals [3]. Besides, DNA damage detection is used in the fields of ecotoxicology, molecular epidemiology, and genotoxicology. There are different methods to evaluate DNA damage. Amongst, comet assay or single-cell gel electrophoresis is the widely used and accepted analysis. The method is based on the microscopic evaluation of the electrophoretic mobility of DNA obtained from a single cell and its nucleus. In general, DNA and/or intact nucleus is isolated, and embedded in thin layers of agarose gel on a slide. The DNA in the agarose gel layers is moved in an alkaline electrophoretic environment. In alkaline media, the chromatin structure opens, and the DNA is partially denatured. Because of the effect of genotoxic factors, single and/or double-strand DNA breaks and DNA fragments of different molecular weights occur. Following electrophoresis, the DNA in the gel is labeled with a fluorescent DNA specific dye like ethidium bromide or silver-stained and observed by a microscope. Intact supercoiled chromatin DNA moves very slowly and observed spherical under the microscope. Depending on the extent of damage, DNA fragments of varying sizes move at differentially with respect to their molecular weight. This results in a form similar to a "comet" in fluorescence microscope images [2,4,5].

Comet assay analysis is the most used method in genotoxic studies due to its high sensitivity. This method also enables the detection of DNA damage in small sample sizes. Besides, it is cheap, reproducible method with short protocol duration [3]. Comet assay images are visually scored by expert researchers from 0 to 4 according to DNA damage levels. However, this scoring needs personal expertise and it may give subjective results.

* Corresponding author.
E-mail addresses: aerdamar@baskent.edu.tr (A. Erdamar), maksahin@baskent.edu.tr (M.F. Aksahin).

https://doi.org/10.1016/j.bspc.2019.101672
1746-8094/

In recent years, few studies have been made in the literature on the classification of these images [3,6–15]. In the proposed study, unlike from the literature, comet scores were classified using the convolution neural network (CNN) method as a deep learning algorithm. Thus, objective and robust results were tried to be obtained by classifying the comet scores successfully. Also, the success of the deep learning algorithm in the classification of cell images was analyzed.

1.1. Related works

Detection of DNA damage is a very important issue in comet assay. However, there are few studies about fully automated computer-aided detection of DNA damage. Furthermore, there is no study or developed algorithm for fully automatic segmentation and DNA damage scoring using CNN in the literature.

Turan et al. combined dynamic time warping method and decision tree in a software program to measure DNA damage and to score it. In their study, each single comet assay was manually extracted, then the center of comet head was marked with giving different scores (Score 0, Score 1, Score 2, Score 3) [16]. Mani et al. proposed a standalone tool named "CoMat" for the detection and quantification of the DNA damage by using a software program developed with Visual Studio. CoMat can process different scores of image formats such as JPEG, TIFF, BMP, and PNG [17]. Ganapathy et al. proposed an automated software to detect and quantify the DNA damage by analyzing comet assay images. Support vector machine method is used to classify images into two groups. These groups are Class 1 and Class 2 that are silver-stained images with lightly or moderately damaged cells and silver-stained images with heavily damaged cells respectively [18]. Quintana et al. used automated comet assay analysis by using an image processing algorithm. In preprocessing step unsharp mask is done. Segmentation was performed using a learning algorithm. After performing several tests, it was determined that the most efficient algorithm was the K-Means cluster based on the spatial relationship of neighboring pixels and the general techniques of object detection with thresholding [19]. Sreelatha et al. developed an automated algorithm to analyze DNA damage using silver-stained comet assay for clinical applications. In the preprocessing stage, a contrast enhancement method is used. Then Gaussian filtering is applied to the contrast-enhanced image. After that Otsu's method is evaluated for the segmentation stage. The comet has separated into three regions. These regions are comet head, tail, and background. In this method, the edges of this region cannot be defined clearly. Therefore, the fuzzy-based algorithm is adopted for clustering [20]. Sreelatha et.al proposed a shading correction algorithm using morphological bottom-hat or top-hat transformation as a preprocessing step. A homomorphic filtering is applied to overcome the problem of silver-stained comet assay the tail region that merged with the background. Then the Otsu method is used to convert binaries image. During morphological filtering operations: morphological closing operation is used to find highly damaged cells and also opening algorithm is evaluated for eliminating noise in the background [14]. Kızıltan et al. proposed a semi-automatic comet assay analysis tool to obtain reliable and accurate measurement results. In this analysis, the head of the comet is segmented from the tail with using the tail moment [6]. Gyori et al. developed a method to detect comets based on geometric properties. They also tried to segment the comet heads using image intensity. Head segmentation of comet is done for lightly damage or no tail DNA since heavily damaged cell tail has a geometrically larger area than the head [10]. Vojnovic et al. focused on algorithms, based on delineating the head from the tail of a comet. This procedure allows detecting very low level of DNA damage. For this purpose, a threshold level is used on the normalized image to determine all bright objects. This threshold level is calculated from the intensity value of the histogram maximum frequency. This procedure can segment the whole area of comet including with both heads and tails together [21]. Gonzalez et al. applied an open-source software, CellProfiler, to analyze automatically comet on the digital image. The boundary of the comet is determined manually. Then, the CellProfiler calculate automatically the measurements of tail and head areas [22]. Sansone et al. developed a comet assay analysis algorithm for minimizing user interaction and for getting more reproducible measurements. The developed algorithm is divided into two steps. In the first step, the comet is detected with Gaussian filtering and morphological operator. In the second step, the comet is segmented as head, halo, and tail with fuzzy clustering to identify areas [7]. Helma et al. proposed an open-source program to analyze the comet assay [12]. Bocker et al. described an automatic image analysis system including software and hardware together to get minimum human interactions. The comet assay image analysis is evaluated in a two-step. These are the automatic comet classification and the calculation of related parameters [9].

2. Material and methods

2.1. Cell and image properties

The comet assay images used in this study were obtained from mammary carcinoma MCF-7 cells. Cell images were obtained by fluorescence microscopy (Nikon, Eclipse E600). 500 comet assay cell images at total were analyzed. Each image was in RGB format and 150×150 pixel size. These dimensions were chosen to cover the area from the head to the tail end of the Comet in each image.

2.2. Image analysis algorithm

The block diagram of the proposed method used in the study is shown in Fig. 1. The algorithm was evaluated by MATLAB(R), The Math Works Incorporation and software using Intel(R) Core(TM) i7 CPU at 1.90 GHz microprocessor, 8.00GB RAM and 64-bit system.

2.2.1. Convolution neural networks

Deep learning techniques enable computers to detect complex layouts in large data sets. The main purpose of the mathematical models created by deep learning techniques is to disseminate the learned expertise and to convey accurate predictions for new and unprecedented data. An artificial neural network consists of connected and arranged in layers called neurons. These layers can be listed as the input layer that the data enter into the network, the hidden layers that convert the data, and the output layer that produces the predictions of the neural network. One-dimensional node graphs of these structures used in medical imaging are shown in Fig. 2. The interest of deep learning in medical imaging is usually performed by CNN [23]. CNN is a type of feed-forward neural networks. CNN is applied to analyze visual imagery. This is because CNN is a powerful method for learning the useful representation of images and other structured data. The node graph applied to the medical images for CNN's is also shown in Fig. 2d. In this figure, the blue dots represent the entrance, the orange dots are hidden, and the green dots represent the output layers [24]. CNN, a specific score of artificial neural networks, aims to maintain spatial relationships in the data with very little connection between layers. The input of the CNN is set in a grid structure and then sent to the layers that protect these relationships. Each layer operation runs in a small region of the previous layer (Fig. 3).

In general, comet images are a two-dimensional matrix. However, a large number of parameters are needed to specify a network. CNN is proposed to reduce these parameters and to adapt the net-

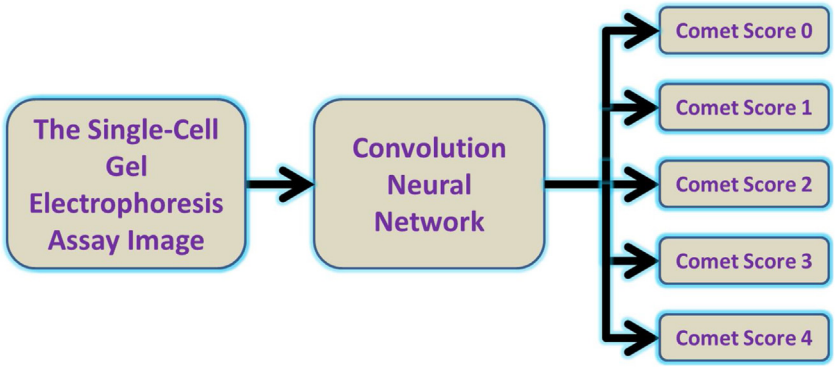

Fig. 1. Block Diagram of comet assay cell scoring.

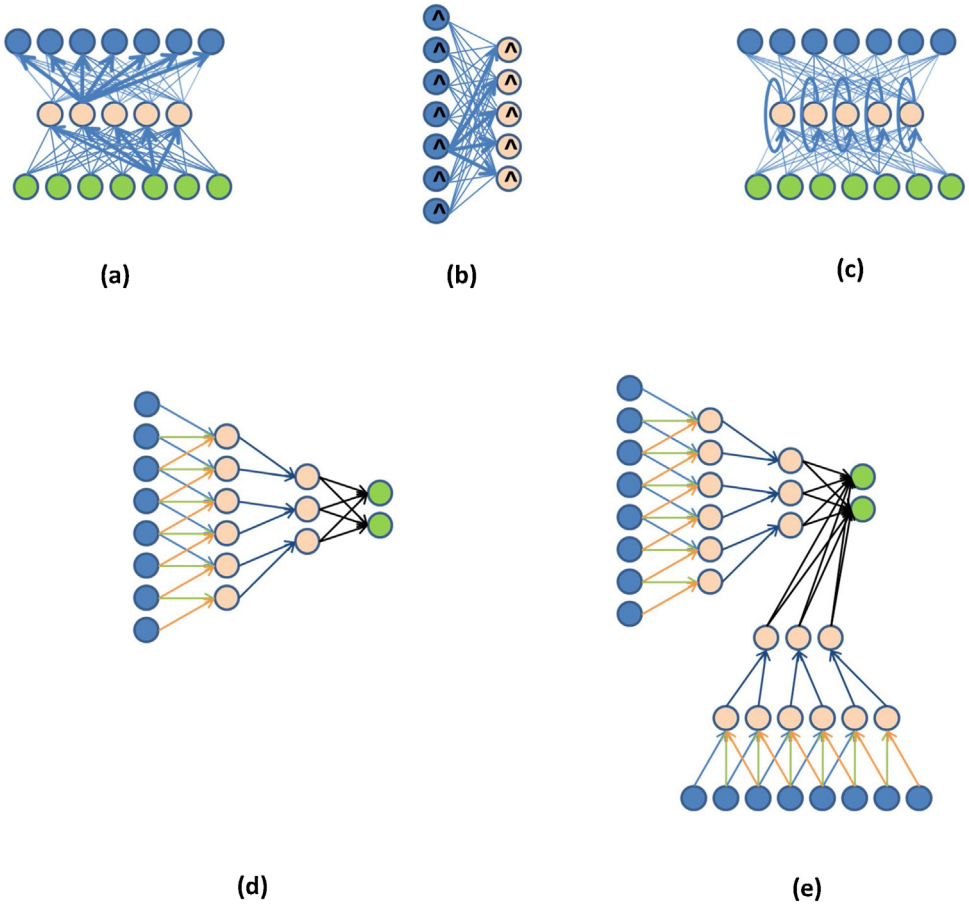

Fig. 2. Node representation of neural networks used in medical imaging a) Auto-encoder, b) Boltzmann model with restriction, c) Recurrent neural networks, d) Convolution Neural Networks, e) Multi-flow folding neural networks.

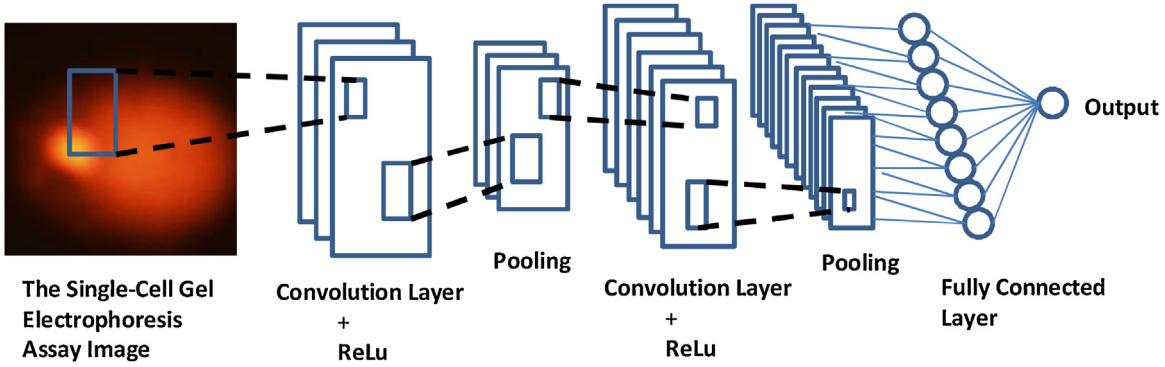

Fig. 3. Simplified representation of CNN structure for the proposed study.

work structure. CNN's are constructed by different layers. These layers differ from their functionalities (Fig. 2).

CNN contains generally three layers. These are input, an output, and multiple hidden layers. The hidden layers are typically consisting of four different types of layers. These are convolution layer, activation layer, pooling layer, and fully connected layer [25].

2.2.1.1. Convolution layer. The general formula of convolution operation is shown in Eq. (1).

$$s(t) = \int x(a)\, w(t-a) da \tag{1}$$

Here x(t) is a continuous-time signal and w(t) is time-domain weighted function.

For the two-dimensional image I, two-dimensional kernel K is needed to make a convolution shown in Eq. (2).

$$S(i,j) = (I * K)(i,j) = \sum_m \sum_n I(m,n) K(i-m, j-n) \tag{2}$$

It can also be written in Eq. (3).

$$S(i,j) = (K * I)(i,j) = \sum_m \sum_n I(i-m, j-n) K(m,n) \tag{3}$$

The CNN input is a matrix form. The dimension of input matrix is (number of images) × (image width (W)) × (image height (H)) × (image depth (D)). Here W and H are the numbers of convolution kernels. W and H are also called hyper-parameters. And D is the kernel depth. In these layers, convolution operations are applied to the input. Then the result is the input of the next layer. Each neuron convolution processes data only for its receptive field. As a result, huge numbers of neurons are necessary because of the large input sizes related to images [26].

$$\text{Input size}: W_1 \times H_1 \times D_1 \tag{4}$$

$$\text{Output volume size}: W_2 \times H_2 \times D_2 \tag{5}$$

where:

$$W_2 = (W_1 - F + 2P)S + 1 \tag{6}$$

$$H_2 = (H_1 - F + 2P)S + 1 \tag{7}$$

$$D_2 = K \tag{8}$$

Here K is the number of filters. F is their spatial extent. S is the stride and P is the number of zero-padding.

2.2.1.2. Activation layer. This activation is used for increasing the non-linearity of CNN without changing the receptive fields of convolution layer. In this layer usually Rectified Linear Unit (ReLU) function is preferred because the training time is faster (shown in Eq. (9)). There are also Leaky ReLU, Randomized Leaky ReLU, Parameterized ReLU, Exponential Linear Units (ELU), Scaled Exponential Linear Units, Tanh, hardtanh, softtanh, softsign, softmax, softplus. In this study, ReLU activation layer, shown in Eq. (9), was used. Because, CNN can be trained much faster. And there is no significant penalty to generalization accuracy [27].

$$f(x) = \max(0, x) \tag{9}$$

A special activation layer, sofmax, is usually used at the end of fully connected layer outputs. This activation layer produces a discrete probability distribution vector [26].

$$P(y = jx) = \frac{e^{x^T w_j}}{\sum_{k=1}^{K} e^{x^T w_k}} \tag{10}$$

Here, x is the sample input vector input and w_j is vectors weight for the predicted probability of y = j.

2.2.1.3. Pooling layer. CNN's pooling is a kind of non-linear down-sampling. There are lots of operations to evaluate pooling. The most commonly used operation is max pooling. In this layer, the input is separated into non-overlapping rectangle parts. Therefore the pooling layer will reduce the spatial size of the input image. It will also reduce the number of parameters, memory footprint, amount of computation and control overfitting. This layer separately acts on every depth slice of the input and resizes it spatially. Generally, the filter sizes are chosen small (size 3×3 or 5×5). Larger filter sizes are also used such as (7×7) but rarely and only in the first convolution layer. Having more small filters is an easy way to achieve high representational power using a smaller number of parameters. It's also suggested to use a small stride to get all useful information in the feature maps, and a zero-padding that keeps the output volume's height and width equivalent to the input volume's height and width [26].

2.2.1.4. Fully connected (FC) layer. The FC layer is a regular structure of an artificial neural network. It is usually seen in the final learning phase. This layer maps the extracted visual features to the desired outputs. Classifications can be done in this layer. The general output of this layer is a vector. Then the output vector is the input of softmax to validate the classifications.

2.3. Performance metrics

The comet assay images, classified using CNN, were scored by expert researchers. The comet assay scores for this classification are accepted as the gold standard. Therefore the performance of the CNN is evaluated according to these scores. The performance metrics of the CNN is determined with calculating the sensitivity, specificity and accuracy values. These metrics are defined as follows:

$$\text{Sensitivity} = \text{TP}/(\text{TP} + \text{FN}) \tag{11}$$

$$\text{Specificity} = \text{TN}/(\text{TN} + \text{FP}) \tag{12}$$

$$\text{Accuracy} = (\text{TP} + \text{TN})/(\text{TP} + \text{TN} + \text{FP} + \text{FN}) \tag{13}$$

Here, true positive (TP) is the number of true classified actual comet assay score that is scored by researchers. False-negative (FN) is the number of wrongly classified comet assay scores. The false positive (FP) is the number of classification in case the actual comet assay score is determined for different comet assay scores. And true negative (TN) is the number of correct scored images while there is no actual comet assay score [28].

3. Results

In this study, 500 single-cell gel electrophoresis assay images were used; equally, consist of five different scores. The representative images of five different comet assay scores are shown in Fig. 4. Fifty percent of all images were used for training, and the rest of the images were used for testing. The trained images were not used for testing. In the training image set, there were 50 images of comet assay score 0, 50 images of comet assay score 1, 50 images of comet assay score 2, 50 images of comet assay score 3, and 50 images of comet assay score 4. The test image set was also equally distributed. Each image has was annotated by the expert researchers as score 0, score 1, score 2, score 3, and score 4.

In this research, various filters sized and numbered CNN structures were trained for classification of the comet assay scores. For all architecture, padding was set to 1, and the stride was set to 2. To show the effectiveness of the CNN classification, the performance metrics, sensitivity, specificity, and accuracy, were calculated. Table 1 shows the training results for constant filter

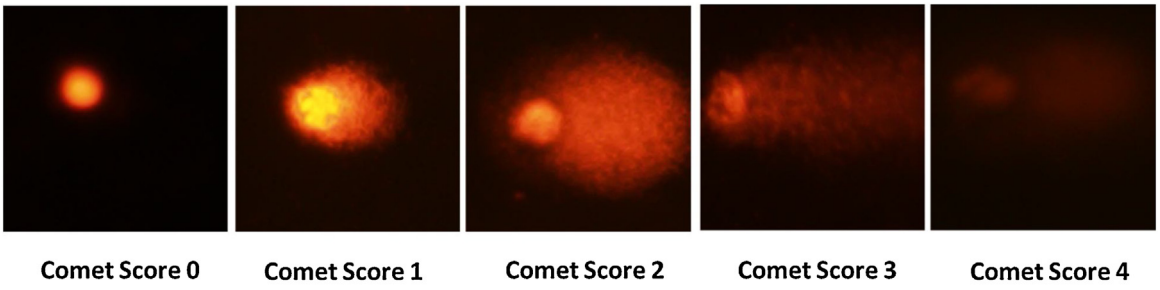

Fig. 4. Five Different Comet Scores.

Table 1
Training results of the overall system accuracy while the number of the filter is 64.

Filter size	2 × 2	3 × 3	4 × 4	5 × 5
accuracy	98.08	100	100	100

Table 2
Test results while the number of the filter is 64.

Filter size	Score of Comet	TPR(sens)	TNR(spec)	ACC(accuracy)
2 × 2	comet score 0	80.8	95.7	92.4
	comet score 1	85.3	93.5	91.1
	comet score 2	84.7	94.7	91.1
	comet score 3	65.2	93.4	90.7
	comet score 4	25.0	98.2	95.8
3 × 3	comet score 0	84.6	96.7	94.1
	comet score 1	79.4	95.2	90.7
	comet score 2	85.9	94.0	91.1
	comet score 3	73.9	93.0	91.1
	comet score 4	75.0	98.7	97.9
4 × 4	comet score 0	88.5	97.3	95.3
	comet score 1	76.5	95.8	90.3
	comet score 2	89.2	91.5	90.7
	comet score 3	69.6	93.4	91.1
	comet score 4	62.5	99.1	97.9
5 × 5	comet score 0	84.6	96.2	93.6
	comet score 1	72.1	96.4	89.4
	comet score 2	89.2	91.5	90.7
	comet score 3	69.6	93.4	91.1
	comet score 4	87.5	98.2	97.9

Table 3
Training results of the overall system accuracy while filter size is 3 × 3.

Number of filters	8	16	32	64	128	256
accuracy	93.27	100	99.04	100	100	100

number with different filter size Table 3 shows the results for constant filter size with different filter number. CNN was well trained with respect to Tables 1 and 3. After the training process, CNN was tested. Tables 2 and 4 show the test results for constant filter number, different filter size, and constant filter size, the different filter number, respectively.

As a result, for comet assay score 0, the best sensitivity value is obtained as 88.5% for 4 × 4 filter size and 64 filter number, the best specificity is obtained as 99.5% for 3 × 3 filter size and 32 filter number, and the best accuracy is obtained as 96.6% for 3 × 3 filter size and 32 filter number. For comet assay score 1, the best sensitivity value is obtained as 92.6% for 3 × 3 filter size and 8 filter number, the best specificity is obtained as 97.6% for 3 × 3 filter size and 32 filter number, and the best accuracy is obtained as 92.8% for 3 × 3 filter size and 32 filter number. For comet assay score 2, the best sensitivity value is obtained as 94.1% for 3 × 3 filter size and 32 filter number, the best specificity is obtained as 96.0% for 3 × 3 filter size

Table 4
Test results while filter size is 3 × 3.

Number of filters	Score of Comet	TPR(sens)	TNR(spec)	ACC(accuracy)
8	comet score 0	82.7	98.9	95.3
	comet score 1	92.6	90.5	91.1
	comet score 2	77.6	96.0	89.4
	comet score 3	73.9	93.4	91.5
	comet score 4	62.5	99.1	97.9
16	comet score 0	82.7	98.4	94.9
	comet score 1	83.8	92.9	90.3
	comet score 2	82.4	92.7	89.0
	comet score 3	56.5	96.2	92.4
	comet score 4	75.0	94.3	93.6
32	comet score 0	86.5	99.5	96.6
	comet score 1	80.9	97.6	92.8
	comet score 2	94.1	89.4	91.1
	comet score 3	60.9	95.3	91.9
	comet score 4	75.0	97.8	97.0
64	comet score 0	84.6	96.7	94.1
	comet score 1	79.4	95.2	90.7
	comet score 2	85.9	94.0	91.1
	comet score 3	73.9	93.0	91.1
	comet score 4	75.0	98.7	97.9
128	comet score 0	84.6	98.4	95.3
	comet score 1	80.9	94.0	90.3
	comet score 2	87.1	90.1	89.0
	comet score 3	65.2	94.8	91.9
	comet score 4	87.5	99.1	98.7
256	comet score 0	88.5	98.4	96.2
	comet score 1	82.4	92.9	89.8
	comet score 2	80.0	91.4	87.3
	comet score 3	65.2	93.4	90.7
	comet score 4	75.0	98.7	97.9

and 8 filter number, and the best accuracy is obtained as 92.8% for 3 × 3 filter size and 32 filter number. For comet assay score 3, the best sensitivity value is obtained as 73.9% for 3 × 3 filter size and 64 filter number, the best specificity is obtained as 96.2% for 3 × 3 filter size and 16 filter number, and the best accuracy is obtained as 92.4% for 3 × 3 filter size and 16 filter number. And for comet assay score 4, the best sensitivity value is obtained as 87.5% for 5 × 5 filter size and 64 filter number, the best specificity is obtained as 99.1% for 4 × 4 filter size and 64 filter number, and the best accuracy is obtained as 98.7% for 3 × 3 filter size and 128 filter number.

4. Discussion

The quantitative analysis of the comet assay images is performed manually expert researchers using various image macros (ImageJ etc.). Image analysis software is used to calculate the amount of DNA in the head and tail, and the length of the tail is also measured. Different software metrics are used to quantify DNA damage. In visual scoring, a tail moment of DNA is expressed

as arbitrary units (AU). Nuclei are scored as 0, 1, 2, 3, and 4 by a blinded observer according to the apparent relative proportion of DNA in the tail and head. Each counted nucleus is multiplied by its score, and total scores are expressed [29]. The most important point in the analysis is the correct detection of the comet score, which determines the DNA damage. This determination depends entirely on the visual scoring and professional experience of the researcher. Scoring hundreds of images is a very time consuming and exhausting task. Therefore, it is inevitable to have subjective results.

The main approach in previous studies is to detect DNA damage, to obtain various features from the spatial parameters of the image and to make classification by using these features. In these studies, the methods are negatively affected by the differences in image characteristics. For example, a method that is successful in images obtained with gray staining does not give the same performance in the images obtained by fluorescent staining since the silver-stained images are noisier than the fluorescent stained images. Hence, regular classification methods fail to effectively detect the comet scores.

At the beginning of this study, we noticed that the fluorescent stained comet assay images had variable image properties (contrast, brightness, etc.). Differences in experimental setups or conditional differences among the laboratories could be the possible reasons for these variances. Nevertheless, this is a major problem for a conventional classification algorithm and has been tried to be solved by various pre-processing methods in previous studies. Also, agarose gel-based residues cause various artifacts in images. These artifacts are another problem that needs to be overcome for image analysis algorithms. In order to solve this problem, various manual add-ons could be applied.

In this study, a new computer-aided classification method is proposed to automatically detect the comet scores using a deep learning approach model. It was shown that the five different comet patterns can be characterized by the CNN algorithm. There is no need for any image conditioning or pre-processing step. The results show that this classification method is robust. It also yields reproducible results for different scores of the comet assay. Besides, there is no human interaction during the test procedure. The presented method does not need any meta-rules or any kind of threshold values.

A more comprehensive comparative evaluation of this study with the previous studies is not feasible since almost all similar studies use specific comet assay images and the researcher performing comet analysis is considered as the gold standard for the validation. Besides, there is not any study using the CNN method in the literature.

5. Conclusion

In proposed work, a deep learning-based classification algorithm has been developed for comet (single-cell gel electrophoresis) assay images. The CNN algorithm has high sensitivity, specificity, and accuracy results. Scores of comet assay images are carried out by expert researchers. This may have subjective consequences, and also may differ according to the visual abilities of the experts. This study shows that with the high-performance scoring results, CNN can objectively determine the comet assay scores as a deep learning algorithm. Moreover, this study will be a reference for the successful application of deep learning techniques to classify other kinds of cell images.

Acknowledgments

The Department of Molecular Biology and Genetics, Faculty of Arts and Science, Baskent University is greatly acknowledged for comet assay and images. Prof. Dr. Özlem Darcansoy İşeri is greatly acknowledged for her contribution.

Declaration of Competing Interest

The authors report no declarations of interest.

References

[1] B. Alberts, Molecular Biology of the Cell, 6th edition, Garland Science, New York, 2015.
[2] Y. Dincer, S. Kankaya, DNA hasarının belirlenmesinde Comet assay, Turk. Klin. J. Med. Sci. 30 (4) (2010) 1365–1373.
[3] G. Sreelatha, P. Rashmi, P.S. Sathidevi, M. Aparna, P. Chand, R.P. Rajkumar, Automatic detection of comets in silver stained comet assay images for DNA damage analysis, in: 2014 IEEE International Conference on Signal Processing, Communications and Computing (ICSPCC), IEEE, 2014, pp. 533–538, August.
[4] A.F. Fidan, DNA hasar tespitinde tek hücre jel elektroforezi, Afyon Kocatepe Üniversitesi Fen Ve Mühendislik Bilimleri Dergisi 8 (1) (2005) 41–52.
[5] M. Dikilitas, A. Kocyigit, Canlilarda "tek hücre jel elektroforez" yöntemi ile DNA hasar analizi (teknik not): comet analiz yöntemi, Harran Tarım ve Gıda Bilimleri Dergisi 14 (2) (2010) 77–89.
[6] E. Kiziltan, E. Yurtcu, Semi-automatic scoring tool for comet assay, in: 2015 IEEE 15th International Conference on Bioinformatics and Bioengineering (BIBE), IEEE, 2015, pp. 1–3, November.
[7] M. Sansone, O. Zeni, G. Esposito, Automated segmentation of comet assay images using Gaussian filtering and fuzzy clustering, Med. Biol. Eng. Comput. 50 (5) (2012) 523–532.
[8] K. Końca, A. Lankoff, A. Banasik, H. Lisowska, T. Kuszewski, S. Góźdź, et al., A cross-platform public domain PC image-analysis program for the comet assay, Mutat. Res. 534 (1–2) (2003) 15–20.
[9] W. Böcker, W. Rolf, T. Bauch, W.U. Müller, C. Streffer, Automated comet assay analysis, Cytometry 35 (2) (1999) 134–144.
[10] B.M. Gyori, G. Venkatachalam, P.S. Thiagarajan, D. Hsu, M.V. Clement, OpenComet: an automated tool for comet assay image analysis, Redox Biol. 2 (2014) 457–465.
[11] J.F. Rivest, M. Tang, J. McLean, F. Johnson, Automated measurements of tails in the single cell gel electrophoresis assay, in: Quality Measurement: The Indispensable Bridge between Theory and Reality (No Measurements? No Science! Joint Conference-1996: IEEE Instrumentation and Measurement Technology Conference and IMEKO Tec, IEEE, 1996, pp. 111–114, vol. 1.
[12] C. Helma, M. Uhl, A public domain image-analysis program for the single-cell gel-electrophoresis (comet) assay, Mutat. Res. 466 (1) (2000) 9–15.
[13] T. Lee, S. Lee, W.Y. Sim, Y.M. Jung, S. Han, C. Chung, et al., Robust classification of DNA damage patterns in single cell gel electrophoresis, in: 2013 35th Annual International Conference of the IEEE Engineering in Medicine and Biology Society (EMBC), IEEE, 2013, pp. 3666–3669, July.
[14] G. Sreelatha, A. Muraleedharan, P. Chand, R.P. Rajkumar, P.S. Sathidevi, An improved automatic detection of true comets for DNA damage analysis, Procedia Comput. Sci. 46 (2015) 135–142.
[15] S. Ganapathy, A. Muraleedharan, P.S. Sathidevi, P. Chand, R.P. Rajkumar, CometQ: an automated tool for the detection and quantification of DNA damage using comet assay image analysis, Comput. Methods Programs Biomed. 133 (2016) 143–154.
[16] M.K. Turan, E. Sehirli, A novel method to identify and grade DNA damage on comet images, Comput. Methods Programs Biomed. 147 (2017) 19–27.
[17] U. Mani, P. Manickam, CoMat: an integrated tool for comet assay image analysis, J. Pharm. Sci. Res. 9 (6) (2017) 919.
[18] S. Ganapathy, A. Muraleedharan, P.S. Sathidevi, P. Chand, R.P. Rajkumar, CometQ: an automated tool for the detection and quantification of DNA damage using comet assay image analysis, Comput. Methods Programs Biomed. 133 (2016) 143–154.
[19] Y.L. Quintana, J.G. Zuluaga, S.S. Arango, Automatic algorithm for processing and analysis of images from the comet assay, World Acad. Sci. Eng. Technol. Int. Sci. Index Biomed. Biol. Eng. 11 (5) (2017) 662.
[20] G. Sreelatha, A. Muraleedharan, P.S. Sathidevi, P. Chand, R.P. Rajkumar, Quantification of DNA damage by the analysis of silver stained comet assay images, IRBM 36 (5) (2015) 306–314.
[21] B. Vojnovic, P.R. Barber, P. Johnston, H.C. Gregory, B. Marples, M.C. Joiner, R.J. Locke, A high sensitivity, high throughput, automated single-cell gel electrophoresis ('Comet') DNA damage assay, Phys. Med. Biol. 58 (1) (2013) 15.
[22] J.E. González, I. Romero, J.F. Barquinero, O. García, Automatic analysis of silver-stained comets by CellProfiler software, Mutat. Res. 748 (1–2) (2012) 60–64.
[23] A.S. Lundervold, A. Lundervold, An overview of deep learning in medical imaging focusing on MRI, Z. Med. Phys. 29 (2) (2019) 102–127.
[24] G. Litjens, T. Kooi, B.E. Bejnordi, A.A.A. Setio, F. Ciompi, M. Ghafoorian, et al., A survey on deep learning in medical image analysis, Med. Image Anal. 42 (2017) 60–88.
[25] A. Karpathy, Cs231n convolutional neural networks for visual recognition, Neural Netw. (2016) 1.

[26] N. Buduma, N. Locascio, Fundamentals of Deep Learning: Designing Next-generation Machine Intelligence Algorithms, O'Reilly Media, Inc., 2017.
[27] A. Krizhevsky, I. Sutskever, G.E. Hinton, Imagenet classification with deep convolutional neural networks, in: Advances in Neural Information Processing Systems, 2012, pp. 1097–1105.
[28] T. Fawcett, An introduction to ROC analysis, Pattern Recognit. Lett. 27 (8) (2006) 861–874.
[29] X. Zhao, G. Aldini, E.J. Johnson, H. Rasmussen, K. Kraemer, H. Woolf, et al., Modification of lymphocyte DNA damage by carotenoid supplementation in postmenopausal women, Am. J. Clin. Nutr. 83 (1) (2006) 163–169.